

CHAPTER IV

RESULT AND DISCUSSION

The studied parameters that can effect to diffusion coefficient are API of Lan Krabue crude, pressure, and temperature. Two different APIs of Lan Krabue crude (14.1 and 21.3) were used to test with two different pressures (300 and 700 psi) at two different temperatures (30 and 40°C) by setting the height of crude oil in the reactor equals to 3.1 cm (approximate volume was 100 mL) for every experiment.

4.1 Effect of Initial Pressure to Diffusion Coefficient

Lan Krabue crude, API 14.1 and 21.3 which were used to test at two different initial pressures (300 and 700 psi) and two setting temperatures (30 and 40 °C). For Lan Krabue crude API 14.1, the pressure change with time pass at two initial pressures and 30 °C and are shown in Fig. 4.1 and Fig. 4.2 and at 40 °C shown in Fig. 4.3 and Fig. 4.4. Similarly, the decay of pressure over time passed at two initial pressures for Lan Krabue crude API 21.3 are shown in Fig. 4.5–Fig. 4.6 at 30 °C and Fig.4.7–Fig. 4.8 at 40 °C.

The decay curve looks like an exponential function at which the initial decay period decreased dramatically and after that decreased slowly until reaching its equilibrium. Moreover, from the experimental found that when carbon dioxide diffused into crude oil, the viscosity of oil decreased dramatically when compare with the initial viscosity.

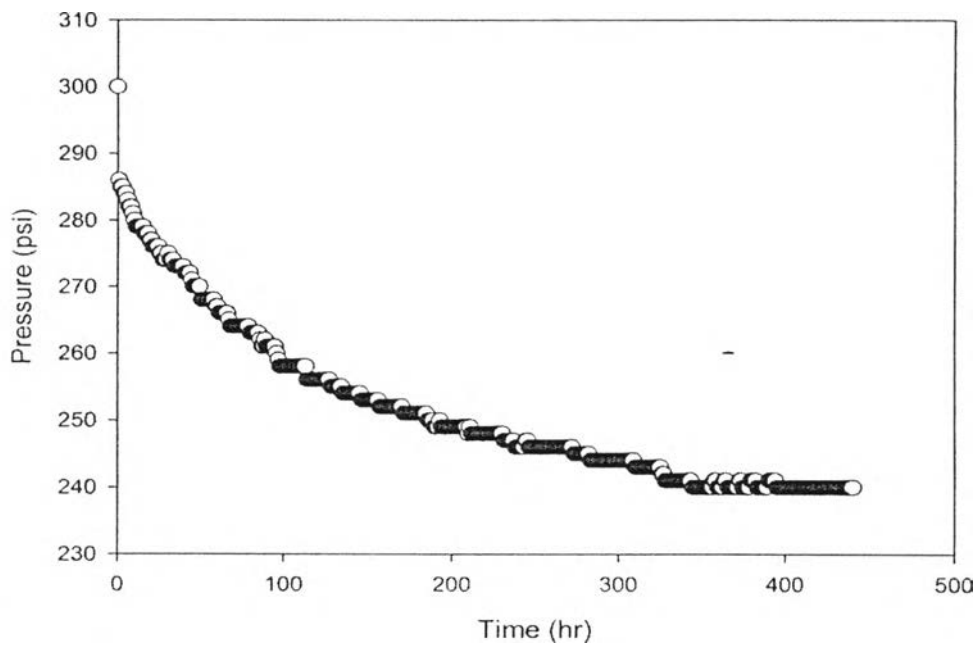


Fig. 4.1 Pressure decay plot for carbon dioxide-crude oil system (API 14.1, $P_i = 300$ psi, $T = 30.46 \pm 0.26$ °C, $Z_0 = 3.1$ cm, CO_2 feed time = 36.5 s. for 440 hr.).

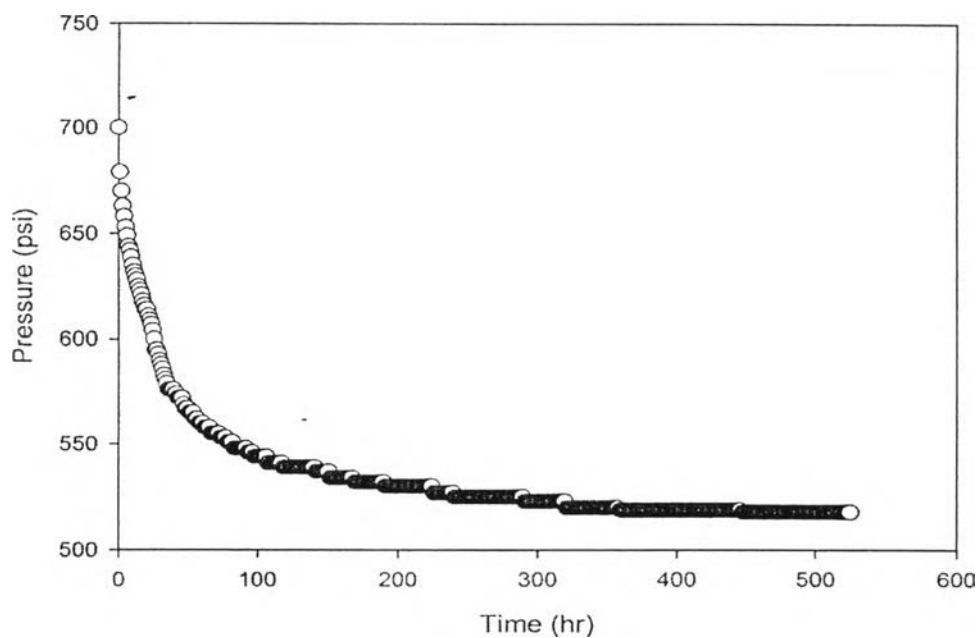


Fig. 4.2 Pressure decay plot for carbon dioxide-crude oil system (API 14.1, $P_i = 700$ psi, $T = 30.39 \pm 0.19$ °C, $Z_0 = 3.1$ cm, CO_2 feed time = 38.2 s. for 525 hr.).

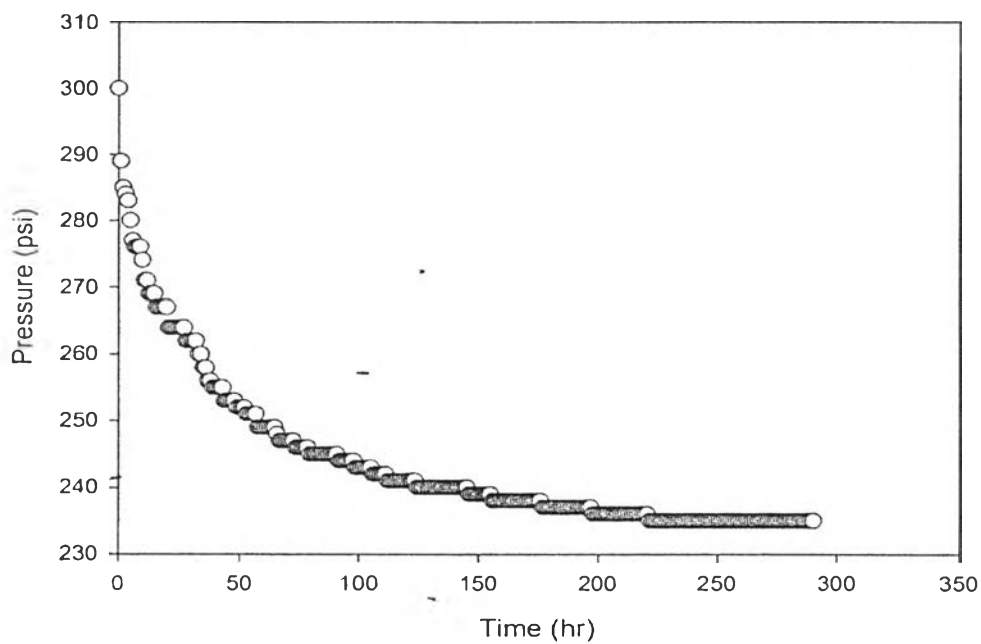


Fig. 4.3 Pressure decay plot for carbon dioxide-crude oil system (API 14.1, $P_i = 300$ psi, $T = 40.27 \pm 0.28$ °C, $Z_0 = 3.1$ cm, CO_2 feed time = 38.3 s. for 290 hr.).

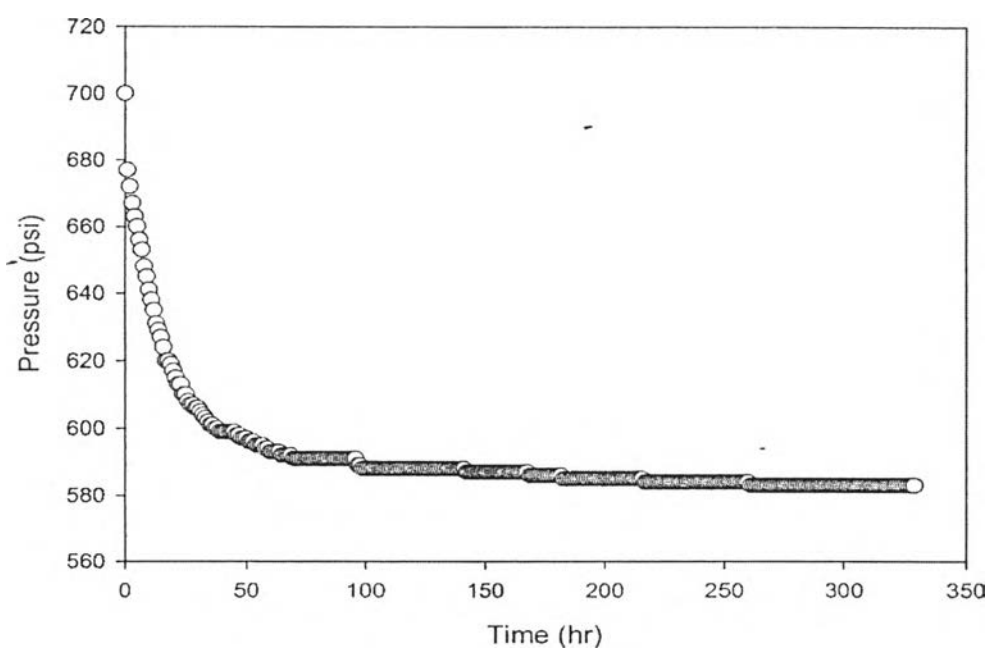


Fig. 4.4 Pressure decay plot for carbon dioxide-crude oil system (API 14.1, $P_i = 700$ psi, $T = 40.22 \pm 0.30$ °C, $Z_0 = 3.1$ cm, CO_2 feed time = 38.9 s. for 329 hr.).

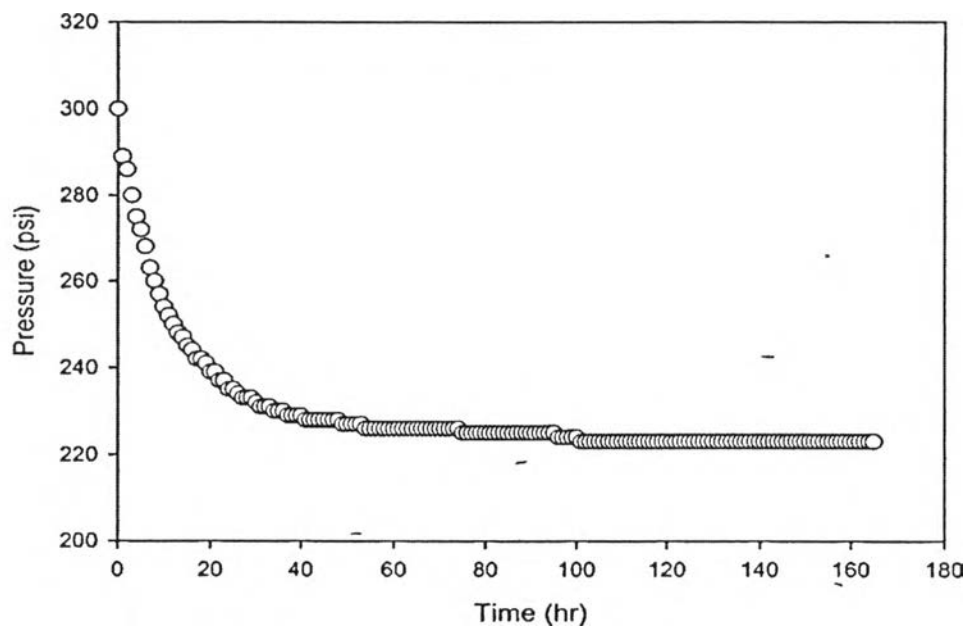


Fig. 4.5 Pressure decay plot for carbon dioxide-crude oil system (API 21.3, $P_i = 300$ psi, $T = 30.40 \pm 0.24$ °C, $Z_0 = 3.1$ cm, CO_2 feed time = 38.4 s. for 165 hr.).

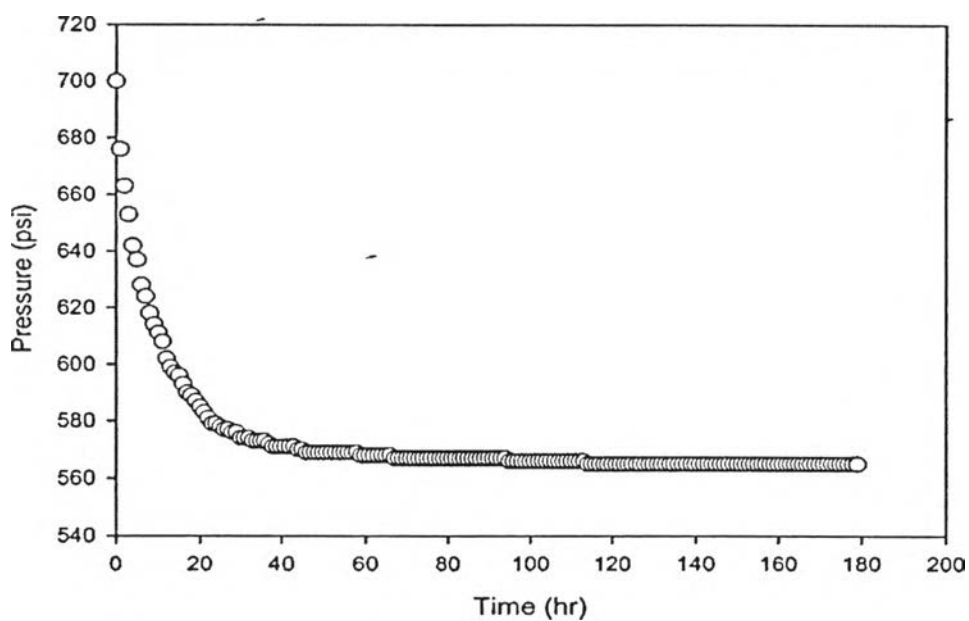


Fig. 4.6 Pressure decay plot for carbon dioxide-crude oil system (API 21.3, $P_i = 700$ psi, $T = 30.42 \pm 0.19$ °C, $Z_0 = 3.1$ cm, CO_2 feed time = 39.2 s. for 179 hr.).

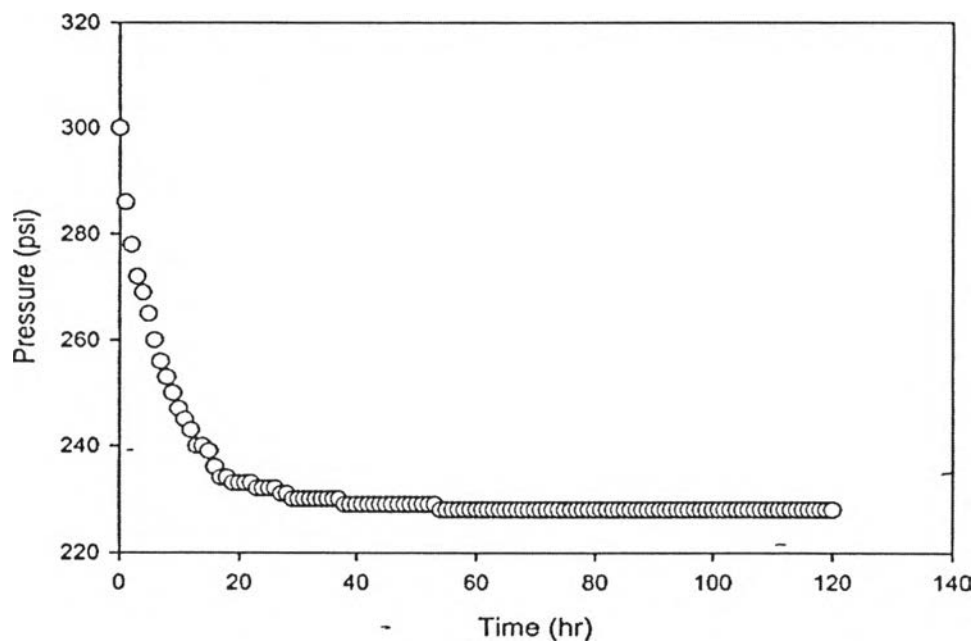


Fig. 4.7 Pressure decay plot for carbon dioxide-crude oil system (API 21.3, $P_i = 300$ psi, $T = 40.26 \pm 0.27$ °C, $Z_0 = 3.1$ cm, CO_2 feed time = 38.9 s. for 120 hr.).

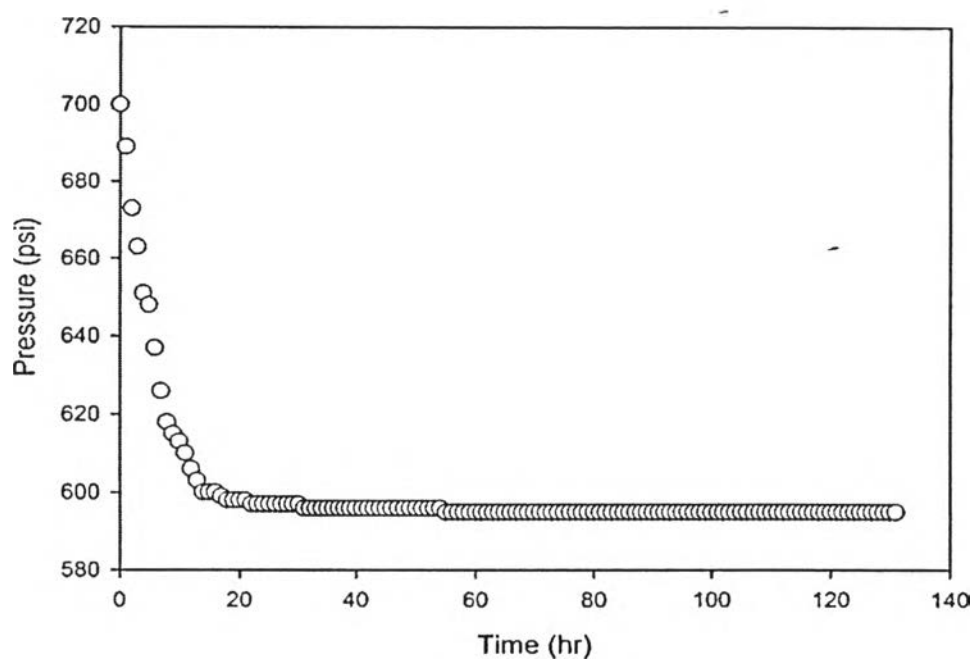


Fig. 4.8 Pressure decay plot for carbon dioxide-crude oil system (API 21.3, $P_i = 700$ psi, $T = 40.20 \pm 0.34$ °C, $Z_0 = 3.1$ cm, CO_2 feed time = 37.6 s. for = 131 hr.).

MATLAB was used to fit the curves of experimental data to measure the equilibrium pressure (P_{eq}) in equation 2.10 by using a curve fitting tool with non-linear regression function following equation 4.1. In equation 4.1, values of a, b, c, and d; the fitting coefficient are taken from MATLAB (equation 4.1) by a and c are m_1 and m_2 in equation 2.10, respectively and the values of b and d can be obtained to calculate k_1 and k_2 in equation 2.10 by substituting the values of b and d into equations 4.2 and 4.3, respectively. Fig. 4.9 to Fig. 4.16 show the fit curve obtained by using equation 2.10.

$$f(x) = a \times \exp(b \times x) + c \times \exp(d \times x) \quad (4.1)$$

$$k_1 = \frac{-1}{b} \quad (4.2)$$

$$k_2 = \frac{-1}{d} \quad (4.3)$$

$$P(t) = m_1 \exp\left(-\frac{t}{k_1}\right) + m_2 \exp\left(-\frac{t}{k_2}\right) + P_{eq} \quad (2.10)$$

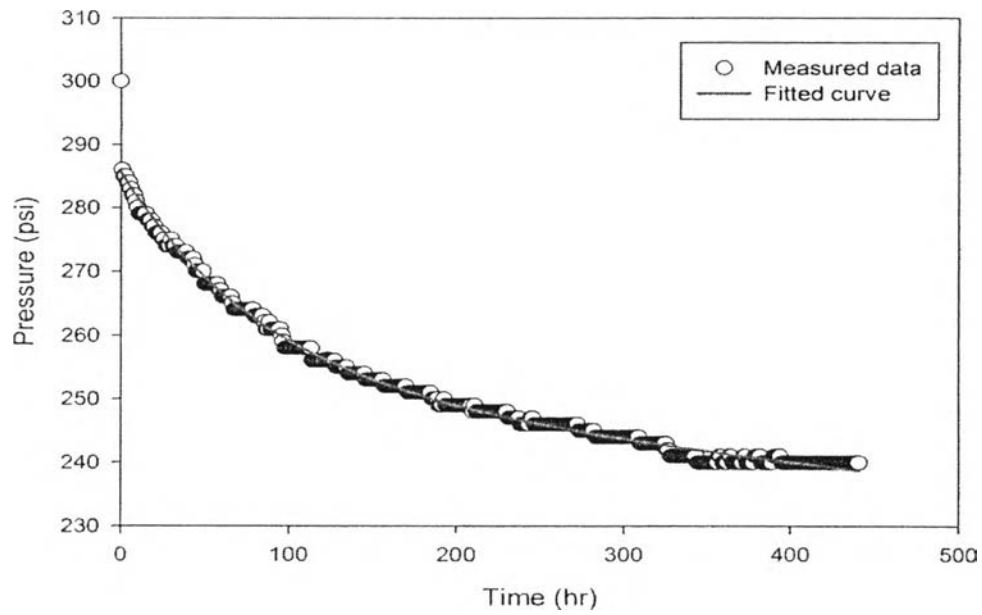


Fig. 4.9 Fitted curve of measured data for carbon dioxide-crude oil system of Fig. 4.1 ($m_1 = 33.64$ psi, $k_1 = 84.746$ hr., $m_2 = 252.00$ psi, $k_2 = 8012.821$ hr., $R^2 = 0.9941$).

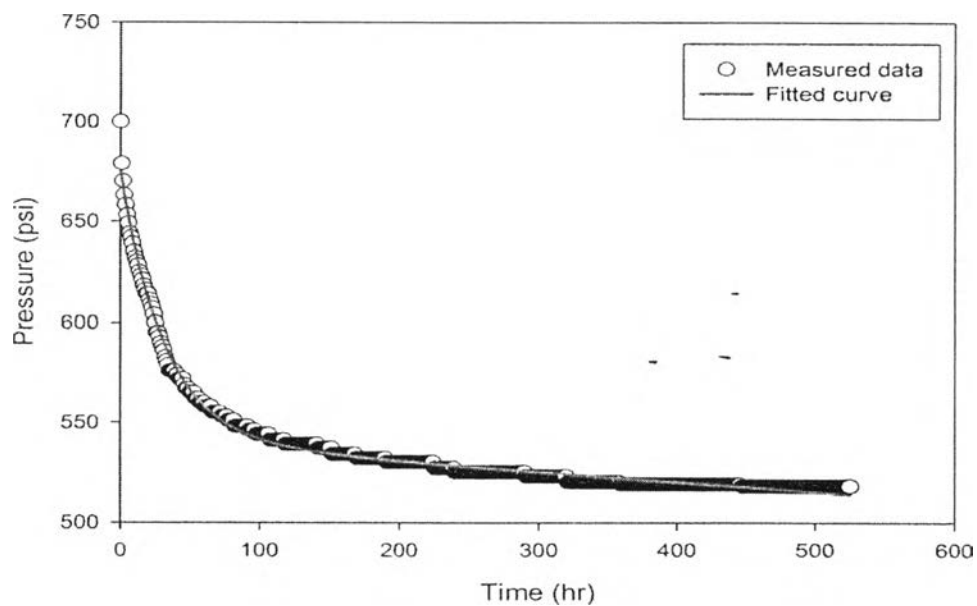


Fig. 4.10 Fitted curve of measured data for carbon dioxide-crude oil system of Fig. 4.2 ($m_1 = 134.30$ psi, $k_1 = 32.072$ hr., $m_2 = 540.80$ psi, $k_2 = 10213.461$ hr., $R^2 = 0.9914$).

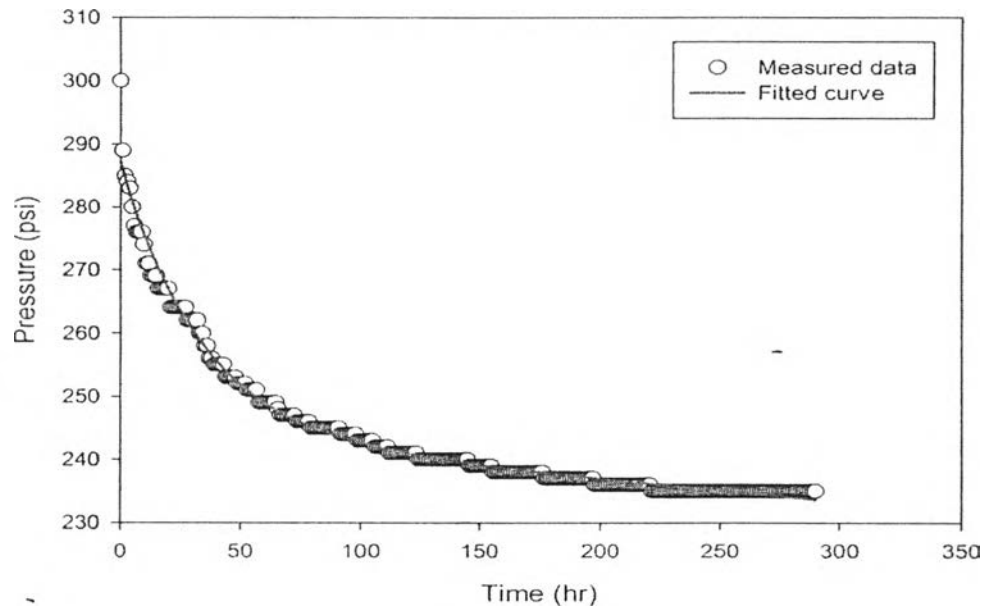


Fig. 4.11 Fitted curve of measured data for carbon dioxide-crude oil system of Fig. 4.3 ($m_1 = 42.92$ psi, $k_1 = 33.289$ hr., $m_2 = 244.20$ psi, $k_2 = 6\,561.680$ hr., $R^2 = 0.9901$).

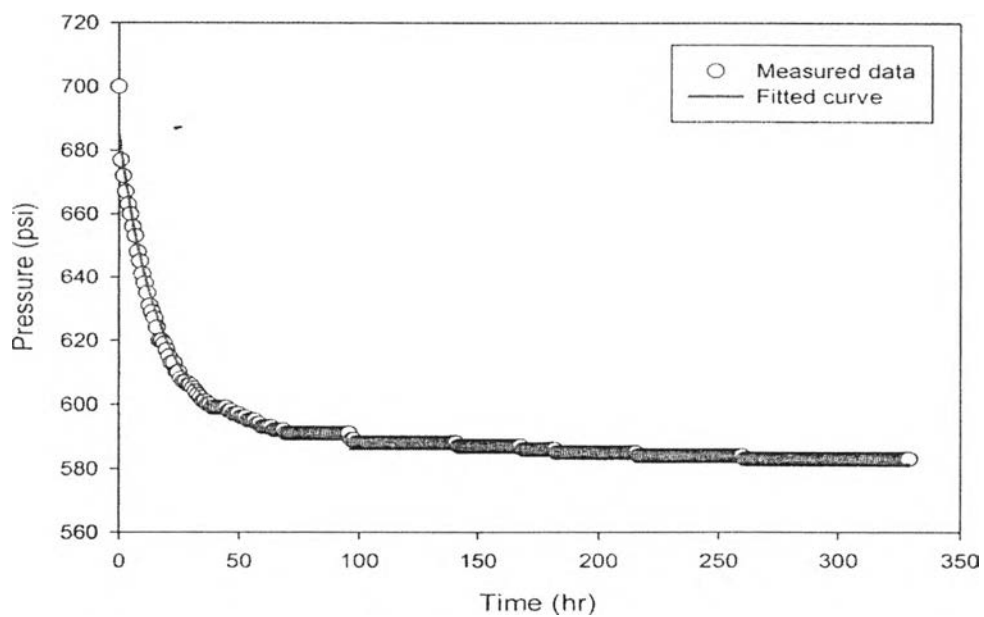


Fig. 4.12 Fitted curve of measured data for carbon dioxide-crude oil system of Fig. 4.4 ($m_1 = 93.44$ psi, $k_1 = 16.764$ hr., $m_2 = 592.10$ psi, $k_2 = 18271.510$ hr., $R^2 = 0.9577$).

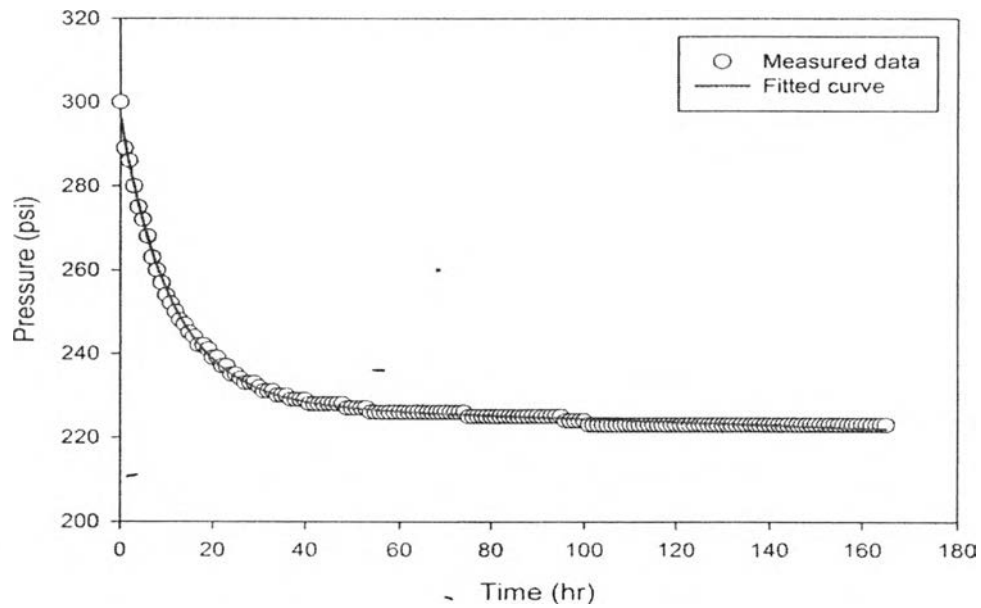


Fig. 4.13 Fitted curve of measured data for carbon dioxide-crude oil system of Fig .4.5 ($m_1 = 68.66$ psi, $k_1 = 11.056$ hr., $m_2 = 228.10$ psi, $k_2 = 6075.334$ hr., $R^2 = 0.9975$).

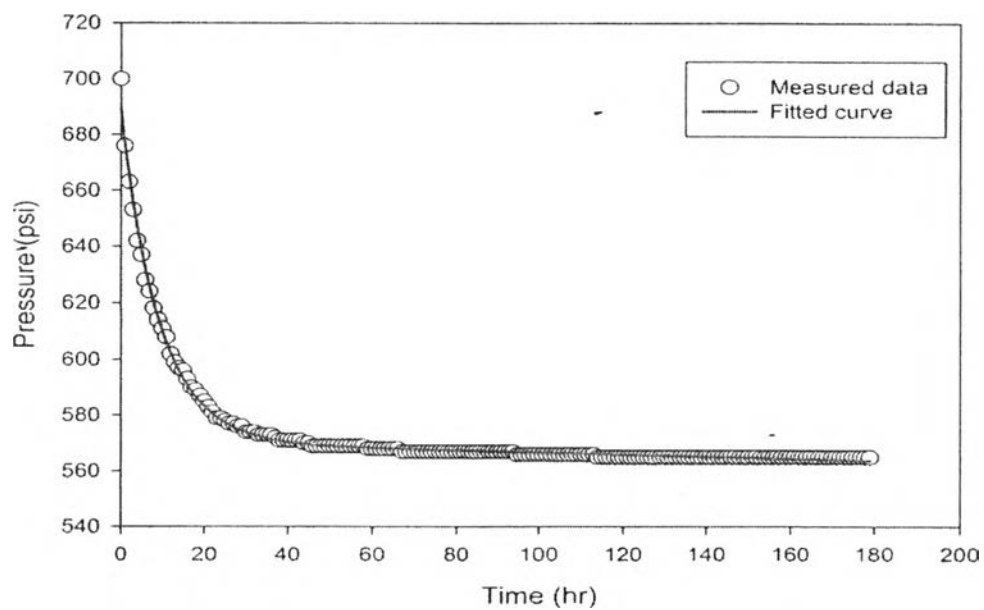


Fig. 4.14 Fitted curve of measured data for carbon dioxide-crude oil system of Fig. 4.6 ($m_1 = 118.7$ psi, $k_1 = 9.234$ hr., $m_2 = 570.40$ psi, $k_2 = 15225.335$ hr., $R^2 = 0.9959$).

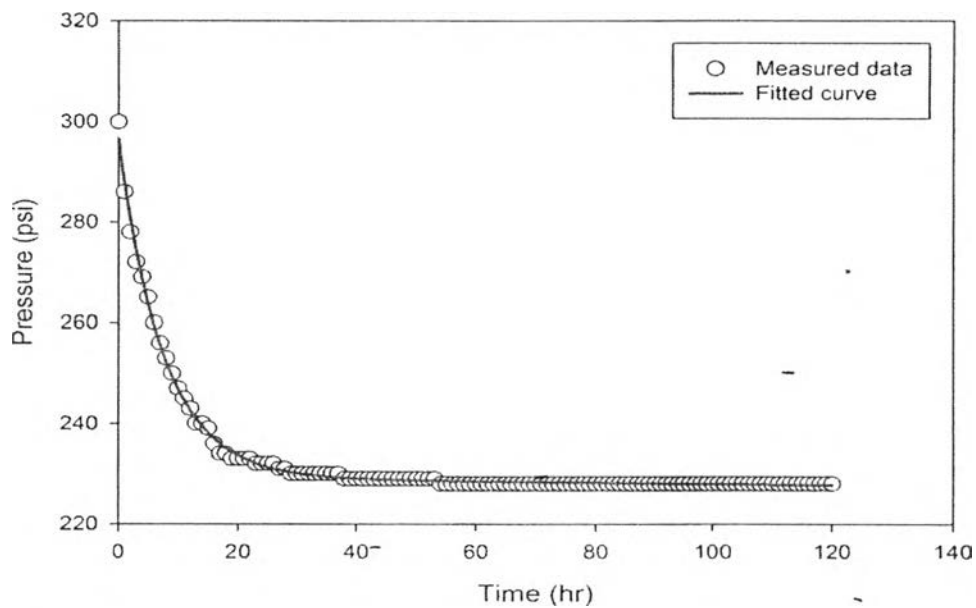


Fig. 4.15 Fitted curve of measured data for carbon dioxide-crude oil system of Fig. 4.7 ($m_1 = 67.32$ psi, $k_1 = 7.491$ hr., $m_2 = 229.20$ psi, $k_2 = 18549.430$ hr., $R^2 = 0.9970$).

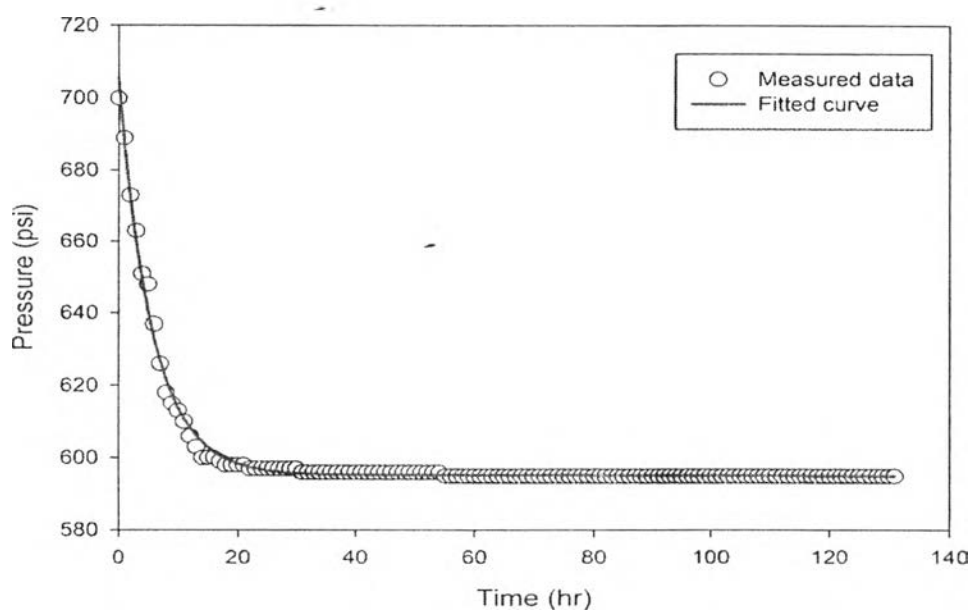


Fig. 4.16 Fitted curve of measured data for carbon dioxide-crude oil system of Fig. 4.8 ($m_1 = 110.2$ psi, $k_1 = 5.609$ hr., $m_2 = 595.30$ psi, $k_2 = 283286.120$ hr., $R^2 = 0.9944$).

The value of k_1 from equation 4.2 was used to calculate the diffusion coefficient of carbon dioxide by substituting k_1 into equation 2.11. For the value of Z_0 set constant at 0.031 meter and the value of π is 3.14, the diffusion coefficient (D_{AB})

$$D_{AB} = \frac{4z_0^2}{k_1\pi^2} \quad (2.11)$$

For the calculation of diffusion coefficient of carbon dioxide, which is calculated as a function of time by using pressure decay method in Lan Krabue crude under the simplifying assumption are applied in Zhang *et al.* (2000) work:

- (i) Swelling of liquid phase is negligible; Z_0 is constant during the test.
- (ii) No resistance to mass transfer at the gas-liquid interface, i.e., the concentration at the interface is the equilibrium concentration.
- (iii) Temperature is constant during the test.
- (iv) The oil is non-volatile liquid.
- (v) The gas phase is single component (pure gas).

Table 4.1 shows the effect of initial pressure on diffusion coefficient of carbon dioxide – crude oil API 14.1 and API 21.3 systems at temperatures at 30 °C and 40 °C, respectively and two different initial pressures of 300 psi and 700 psi.

Table 4.1 Effect of initial pressure on diffusion coefficient of carbon dioxide-crude oil, API 14.1 and 21.3 systems and temperature are constant at 30 °C and 40 °C

Temp (°C)	API	P _i (psi)	Diffusion coefficient, D (m ² /s)
30	14.1	300	1.28×10 ⁻⁹
		700	3.25×10 ⁻⁹
	21.3	300	9.80×10 ⁻⁹
		700	1.17×10 ⁻⁸
40	14.1	300	3.38×10 ⁻⁹
		700	6.46×10 ⁻⁹
	21.3	300	1.45×10 ⁻⁸
		700	1.93×10 ⁻⁸

The diffusion coefficient of carbon dioxide increased significantly with increasing the initial pressure because the driving force of carbon dioxide was increased with its concentration and increased the interaction between carbon dioxide gas and crude (Upreti, 2002 and Song, 2010).

4.2 Effect of Temperature

Lan Krabue crude; API 14.1 and API 21.3 are used to test with two different temperatures (30 °C and 40 °C) and setting pressure constant for each tested initial pressure (300, and 700 psi). Fig. 4.17 and Fig. 4.18 show fitted curve of measured which obtained from MATLAB data for carbon dioxide-crude oil API 14.1 system at 300 psi and 700 psi. And the fitted curve of measured data for carbon dioxide-crude oil API 21.3 system that obtained from MATLAB at 300 psi and 700 psi are shown in Fig. 4.19 and Fig. 4.20, respectively.

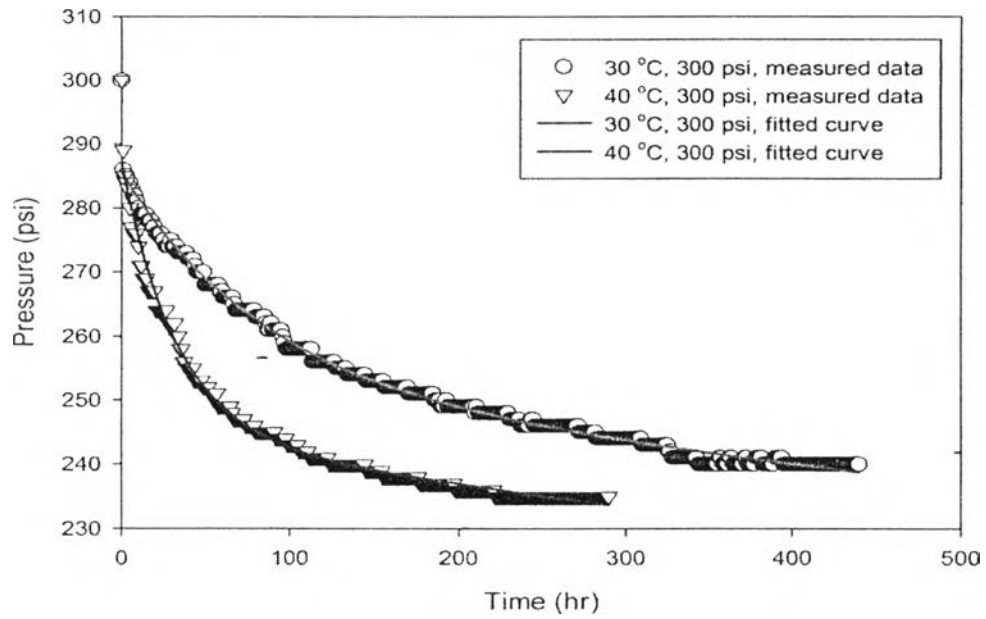


Fig. 4.17 Effect of temperature on pressure decay plot for carbon dioxide-crude oil API 14.1 system at 300 psi.

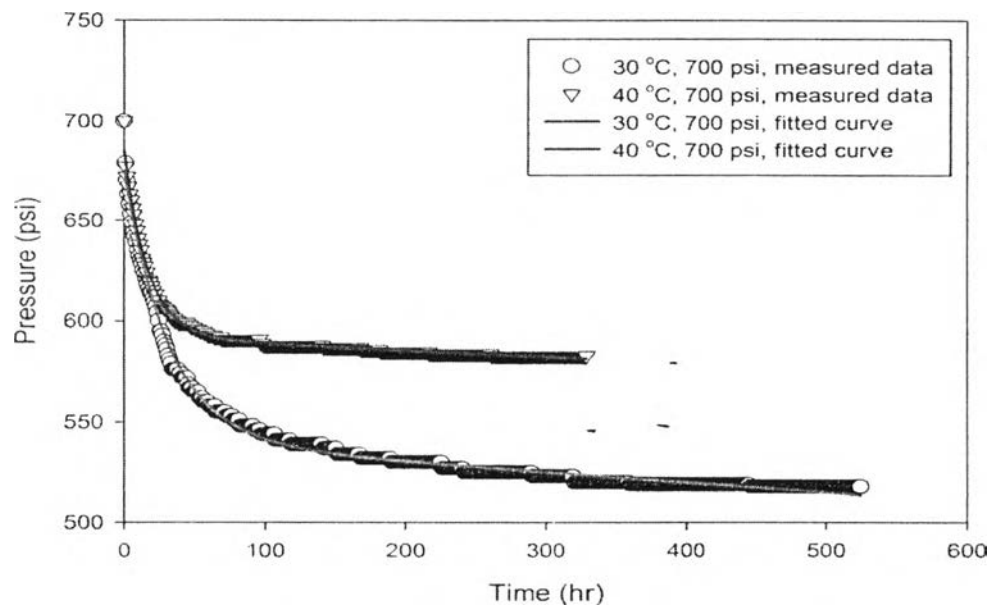


Fig. 4.18 Effect of temperature on pressure decay plot for carbon dioxide-crude oil API 14.1 system at 700 psi.

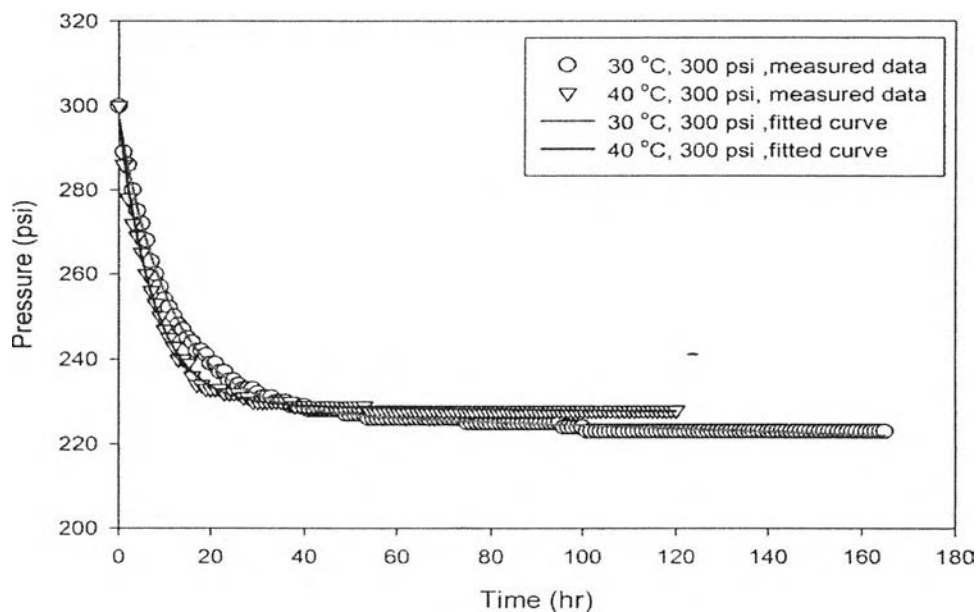


Fig. 4.19 Effect of temperature on pressure decay plot for carbon dioxide-crude oil API 21.3 system at 300 psi.

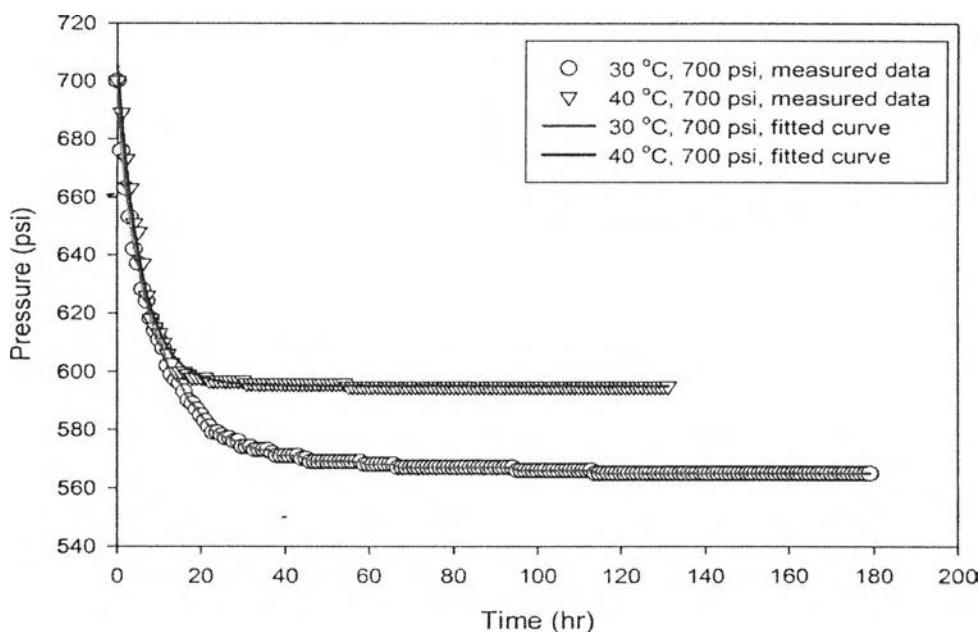


Fig. 4.20 Effect of temperature on pressure decay plot for carbon dioxide-crude oil API 21.3 system at 700 psi.

Fig. 4.17 to Fig. 4.20 reveal that at the same initial pressure, higher temperature has a higher rate of pressure decay than lower temperature

especially in the first period of test. Moreover, the higher temperature can reach the equilibrium pressure faster than the lower temperature at the constant pressure due to its viscosity decreased when temperature increased.

Table 4.2 Effect of temperature on diffusion coefficient of carbon dioxide-oil API 14.1 and 21.3 systems and initial pressure are constant at 300 psi and 700 psi

P_i (psi)	API	Temp ($^{\circ}$ C)	Diffusion coefficient, D (m^2/s)
300	14.1	30	1.28×10^{-9}
		40	3.38×10^{-9}
	21.3	30	9.80×10^{-9}
		40	1.45×10^{-8}
700	14.1	30	3.25×10^{-9}
		40	6.46×10^{-9}
	21.3	30	1.17×10^{-8}
		40	1.93×10^{-8}

Table 4.2 shows the diffusion coefficient of carbon dioxide–crude oil API 14.1 and API 21.3 systems at two different temperatures of 30 $^{\circ}$ C and 40 $^{\circ}$ C and at the initial pressures of 300 psi and 700 psi. The diffusion coefficient at 40 $^{\circ}$ C is higher than the diffusion coefficient at 30 $^{\circ}$ C at constant initial pressure because when temperature increased, the viscosity of crude decreased and thus, carbon dioxide gas can easily penetrate into the crude.

4.3 Effect of API Gravity

The crude oil with API gravities of 14.1 and 21.3 from Lan Krabue were tested with two different initial pressures, 300 psi and 700 psi, and two temperatures of 30 $^{\circ}$ C and 40 $^{\circ}$ C. Fig. 4.21 to Fig. 4.24 show that at the same initial pressure and constant tested temperature, Lan Krabue crude with API 14.1 has a lower rate of

pressure change than that with API 21.3, especially in the first period of test that can be easily observed. Moreover, the higher API gravity reached the equilibrium pressure faster than the lower API gravity at the constant initial pressure and tested temperature due to the decrease of its viscosity.

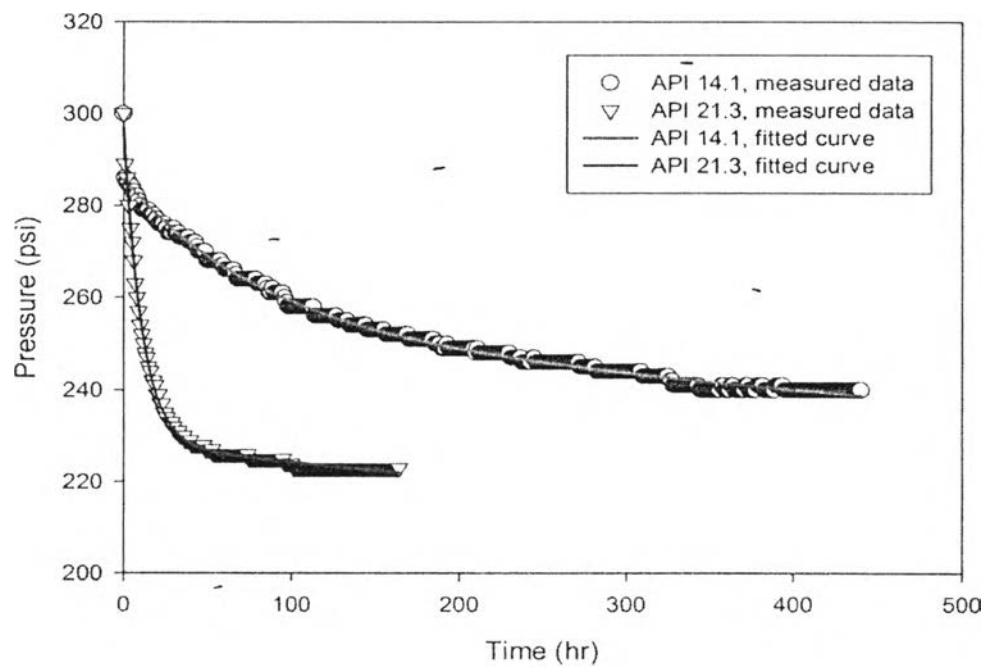


Fig. 4.21 Fitted curve for carbon dioxide-crude oil test at 30 °C and 300 psi.

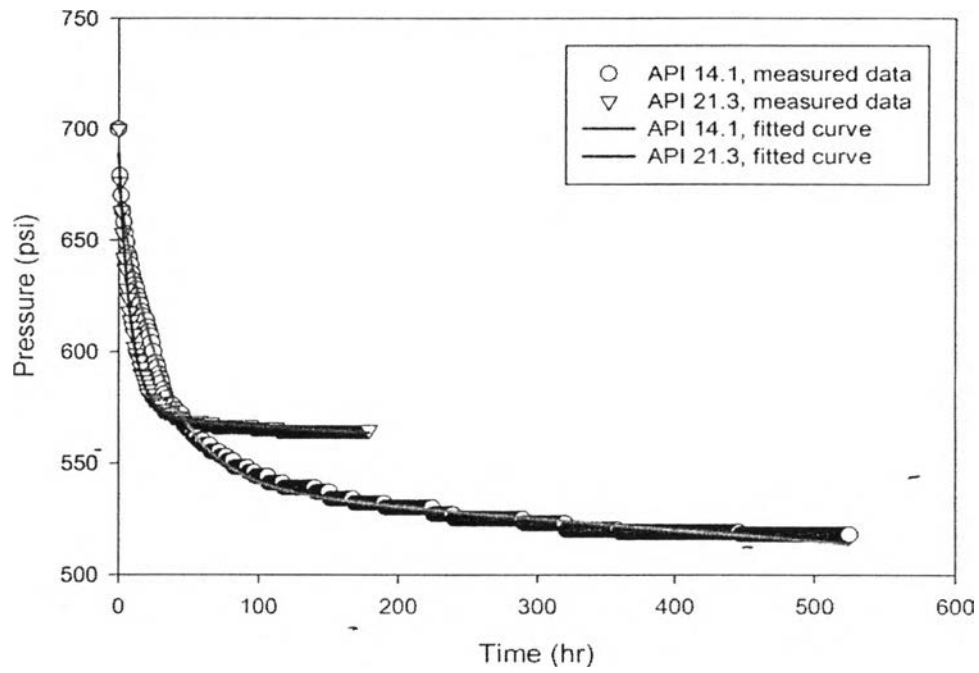


Fig. 4.22 Fitted curve for carbon dioxide-crude oil test at 30 °C and 700 psi.

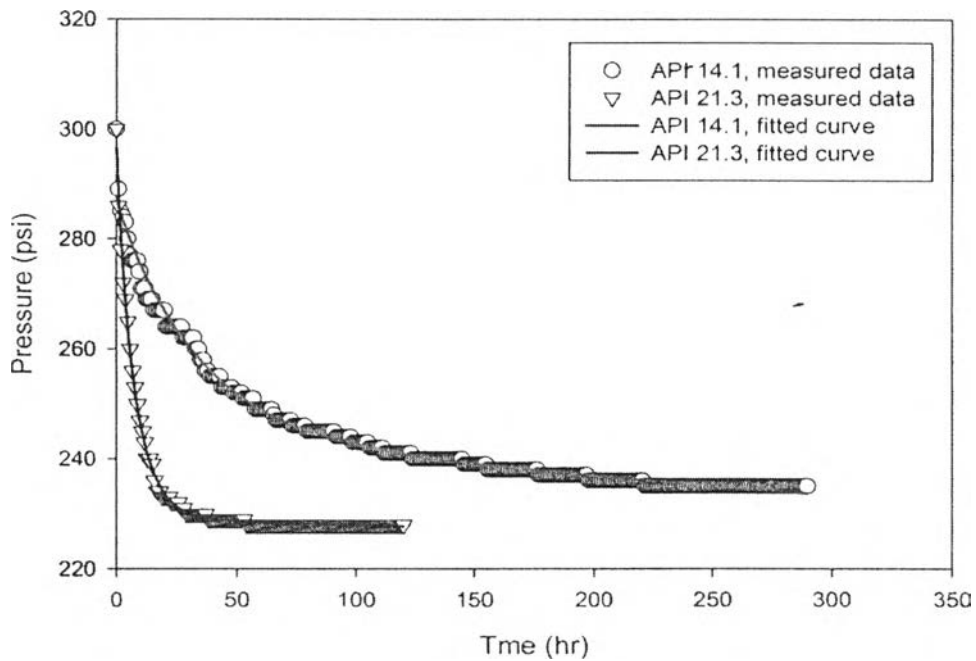


Fig. 4.23 Fitted curve for carbon dioxide-crude oil test at 40 °C and 300 psi.

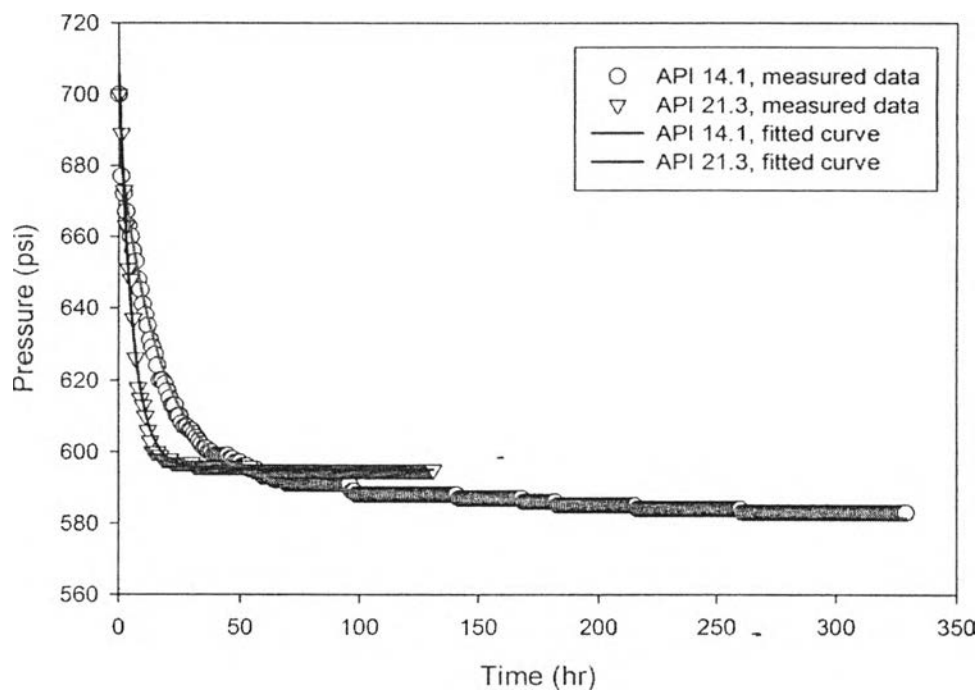


Fig. 4.24 Fitted curve for carbon dioxide-crude oil test at 40 °C and 700 psi.

Table 4.3 shows the effect of API gravity of Lan Krabue crude on diffusion coefficient of carbon dioxide-crude oil API 14.1 and 21.3 systems with two constant tested temperatures (30 °C and 40 °C) and initial pressure is constant at 300 and 700 psi, respectively by using equation 2.11.

Table 4.3 Effect of API gravity on diffusion coefficient of carbon dioxide-oil API 14.1 and 21.3 system with constant temperature, 30 °C and 40 °C and constant initial pressure at 300 psi and 700 psi

Temp (°C)	P _i (psi)	API	Diffusion coefficient, D (m ² /s)
30	300	14.1	1.28×10^{-9}
		21.3	9.80×10^{-9}
	700	14.1	3.25×10^{-9}
		21.3	1.17×10^{-8}
40	300	14.1	3.38×10^{-9}
		21.3	1.45×10^{-8}
	700	14.1	6.46×10^{-9}
		21.3	1.93×10^{-8}

From Table 4.9 to Table 4.12 reveal that the diffusion coefficient increases when increasing the API gravity of crude oil due to the decreasing in viscosity of crude oil makes carbon dioxide can diffuse into the crude easily.